Listening to Temperature: Ultrasonic Non-Destructive Identification of Material Phase and Temperature

Taylor Jeffrey[1,a)], David Jack[1,b)], and David Moore[2,c)]

[1]*Baylor University Department of Mechanical Engineering, Waco, TX, 76798, USA*
[2]*Sandia National Laboratories, Albuquerque, NM, 87123, USA*

a) Taylor Jeffrey: Taylor_Jeffrey2@baylor.edu
b) David Jack: David_Jack@baylor.edu
c) David Moore: dgmoore@sandia.gov

Abstract. In the chemical transport field, such as petro-chemicals or food processing, there is a need to quantify the spatially varying temperature and phase state of the material within a cylindrical vessel, such as a pipeline, using non-invasive techniques. Using ultrasonic signals, which vary in time-of-flight, intensity, and wave characteristics based on the temperature and phase of a material, an automated technique is presented which can provide a non-axisymmetric map of the phase and temperature inside a cylindrical vessel within a single plane using exclusively information from the through-transmission wave and the external temperature profile. This research demonstrates the approach using an amorphous wax, due to its stable nature and ability to be reheated many times without changing the properties of the wax. Due to its amorphous nature, the wax transitions from a solid to a low-viscosity fluid over a range of temperatures. This behavior is similar to that of a thermoplastic and a slurry experiencing curing. As the spatial temperature within a container of wax increases the time of flight for an ultrasonic signal will change. Results presented indicate the ability of the investigated technique to map the temperature and phase change of the wax based solely on the ultrasonic signals and knowledge of the external temperature on the outer edge of the vessel.

INTRODUCTION

In many science and engineering applications, there is a need to characterize the internal temperature distribution within a material as it undergoes thermal gradients, with particular interest given to the range of temperatures near a phase change. Thermocouples are a common solution, however they are an invasive method which may damage the material during insertion or disrupt flow during the phase change, cause non-uniform heating due to their thermal conductive behavior within the structure itself, or have limited use long-term in high-temperature or other hostile environments. Infrared imaging is commonly used for temperature measurement, however it is limited to the surface temperature of the material or container, and cannot provide imaging for internal temperatures. Thermography and temperature mapping using ultrasonics has been researched for many years, and there are several methods and techniques for reconstructing temperature fields for systems containing a single phase of the material based on ultrasound [1-7]. Least squares method is often the baseline for comparison of newer techniques, including radial basis function [1,2]. Computerized tomography is another method used for temperature measurement via ultrasound [5]. The thermal state of the gas within a powerplant boiler has been researched [7] along with systems composed exclusively of a single type of a solid material [6,8], which also has applications in the medical industry [3]. Schmidt et al studied temperature prediction at the interface of a solid and a harsh environment [4], and found it possible to determine surface temperature and a temperature profile within the domain. However there is much research still to be done on a material that spans more than a single material phase state due to the presence of thermal gradients within the system. In addition, this work focuses on a material that does not have a single set temperature for a phase transition such as that of a thermoplastic or similar amorphous materials near their melt temperature zone.

Determining the temperature and phase of materials using non-invasive techniques has immediate applications in the petro-chemical industry, the food industry, and the polymer industry. For example, a pipeline experiencing a loss in efficiency could be monitored to locate a partial blockage and to determine the internal environment and temperature of the pipeline. Ultrasonics have already been used for quality control in food applications [10,11]. And as additive

manufacturing with the Large Area Additive Manufacturing with carbon fiber reinforced polymers and other materials continues to expand [14-16], knowing the internal temperature of an extrusion both before and after it exits the nozzle will allow for continued improvement and modelling.

In this paper, there is a brief overview of ultrasonic theory basics, followed by an explanation of the material selection and characterization process with specific interest given to the correlation between the internal speed of sound of a uniformly heated material as a function of temperature and its correlation to the melt transition region identified using differential scanning calorimetry. The experimental procedure and data collection processes along with an overview of the data processing. Results are then presented for the modeled phase boundary and 2D profile of the internal temperature state of the wax using only the ultrasonic data collected and an assumed temperature profile of the exterior of the testing vessel. The temperature and state identification using ultrasound are then verified against internal thermocouple measurements throughout the entire test and a qualitative comparison is made as a single moment for the phase stated as the characterization of the phase boundary is not readily available.

ULTRASONIC THEORY

Perhaps the most basic form of ultrasonic data comes in the form of an A-scan [17-18], where the acoustic energy captured by a piezo-electric transducer is plotted as a function of time as shown in Figure 2. Through transmission, as depicted in Figure 1, uses two ultrasonic transducers, one on either side of a container, with Transducer T sending the signal and Transducer R receiving the signal. The signal received by Transducer R would typically look something like that shown in Figure 2, a plot of the signal intensity as a function of time.
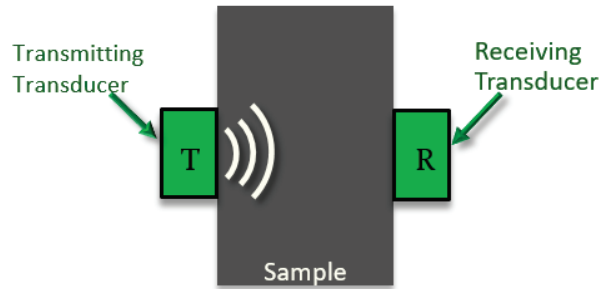

FIGURE 1. Through transmission with a pair of ultrasonic transducers

The time of flight (TOF) is the amount of time between a sound wave being transmitted and received by ultrasonic transducers. In Figure 2a the first visual onset of the signal occurs at 57 μs. This signal onset is often quite difficult to quantify, especially in the presence of a noisy data set, so a user defined threshold is set. This threshold is typically given in terms of a saturation percentage used to detect the onset of the signal corresponding to the transmission wave. To maintain consistency across various amplitude signals, this threshold is defined relative to the peak intensity of the signal itself.
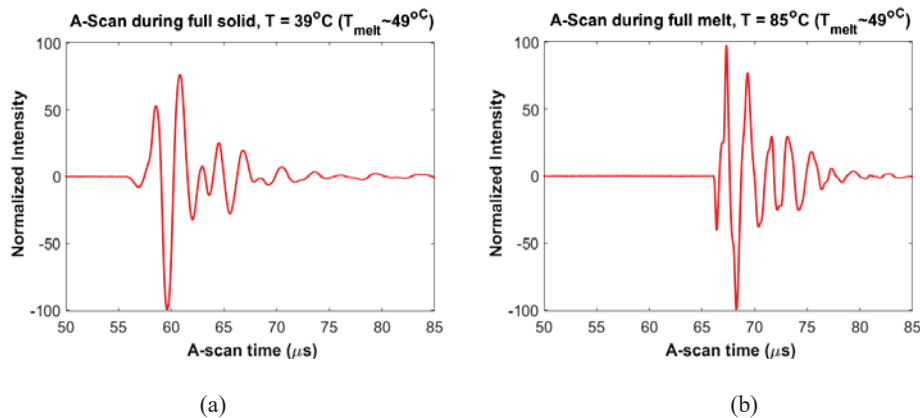

(a)   (b)

FIGURE 2. Signal intensity for (a) fully solid wax and (b) fully melted wax indicating time of flight

Time of flight directly relates to the effective speed of sound (SOS). The distance traveled by the ultrasonic signal divided by the time of flight of the signal is the effective, or bulk, speed of sound. When working with ultrasonic signals, speed of sound is one of the most-used parameters when working with ultrasonic signals.

Time of flight should account for any time spent traveling through container material in order to obtain a more accurate speed of sound. The speed of sound is known to be temperature dependent. In the present study we use the measured time of flight to attain the bulk speed of sound and then compare the results to the speed of sound of the material over a range of temperatures. As will be discussed in the later sections, this requires more detail for a material that is not within a homogeneous temperature state.

Energy is lost as the ultrasonic signal passes through the material, a process known as attenuation. The dissipation, absorption, and ultrasonic scattering of the signal inside the material all contribute to attenuation. To maintain the full signal resolution, an electrical gain is used to amplify the captured waveform. This process increases the amount of energy in the initial signal, which can compensate for energy lost during attenuation.

EXPERIMENTAL SETUP AND PROCEDURE

Material Selection and Characterization

It is crucial to understand the properties and behavior of the material used during experimentation. In this study, we investigate an amorphous wax, known as CBL-125 made by The Candlewic Company. The wax has a low coefficient of thermal expansion, and contracts very little during the transition from a liquid to an amorphous solid. Additionally, CBL-125 is highly attenuative, and that attenuation is a function of temperature. The overall material behavior is similar to that of a thermoplastic and is representative of a polymer undergoing a transition from that of a melt to a rubbery material above the glass transition. All testing is generated and collected with a US Ultratek EUT3160 8-Channel Pulsar/Receiver, paired with Olympus 0.5 MHz/1.0" Transducers. The EUT3160 is operated using a custom LabVIEW virtual instrument. The internal wax temperature is directly measured through embedded K-type thermocouples connected to a Graphtec GL820 Data Acquisition Device.
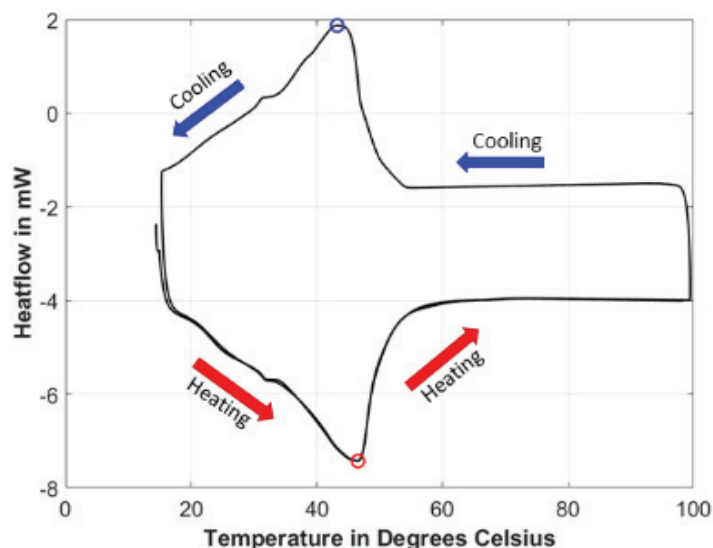

FIGURE 3. DSC curve for CBL-125 at a rate of 5°C/min

The melt temperature is first quantified using Differential Scanning Calorimetry (DSC). A 6.45mg sample of CBL-125 was placed into a TA Instruments Q20 Differential Scanning Calorimeter, and subjected to a heating rate of 5°C/min. The results shown in Figure 3 indicate that during the heating melt initiates a little before 45°C with the peak energy for heating, often corresponding to the greatest change in the material state, occurring at 46.5°C and the wax being fully melted around 50 degrees as defined by the inflection point on the upward slope of the heating curve. During the cooling the transition from liquid to solid again occurs around 50°C with the solidification being completed by 43.2°C. These temperatures were identified by locating the temperatures corresponding to the maximum and minimum heat flow values. It should be noted that CBL-125 does not instantly transition from liquid to solid and vice versa, but that the phase change occurs over a range of temperatures. The heating rate of the DSC testing can affect

which temperature the maximum and minimum heat flow values occur at [11] and so a small shift due to thermal lag is expected on the resulting energy curve during heating and cooling. Thus, the phase change for CBL-125 is expected to lie between 45°C and 50°C.

The authors note that the DSC curve for CBL-125 is similar during the melt transition to that of many thermoplastics, which also have a range of temperatures over which melt occurs [12]. It does differ in that there is not an equivalent concept of a glass transition temperature with the corresponding inflection point for CBL-125.

A second test is performed by heating the wax and then held isothermally at various temperatures above and below the melting temperature range. Notice in Figure 2 that the time of flight for an ultrasonic signal in CBL-125 varies significantly with temperature.

A shorter time of flight is observed when the material is at a lower temperature, as compared to fully melted and heated CBL-125. For the solid wax (Fig. 2a) and the liquid (Fig. 2b) wax, the time of flight is, respectively, 57 μs and 65 μs. The intensity on both plots is normalized to a peak intensity of +/- 100, with the gain for the solid and the liquid test being, respectively 37.5 dB and 21.3 dB. In addition to the temporal and the attenuation shifts, there is also a clear change in the characteristic of the signal as seen between the solid and the liquid. This final characteristic will be highlighted by investigating the frequency characteristics of the signal in the results section.

A speed of sound vs temperature master curve (Figure 4) is created by heating the CBL-125 isothermally and then recording the corresponding time of flight. Observe in Figure 4 that the time of flight increases as the temperature increases causing the speed of sound to decrease as a function of increasing temperature.
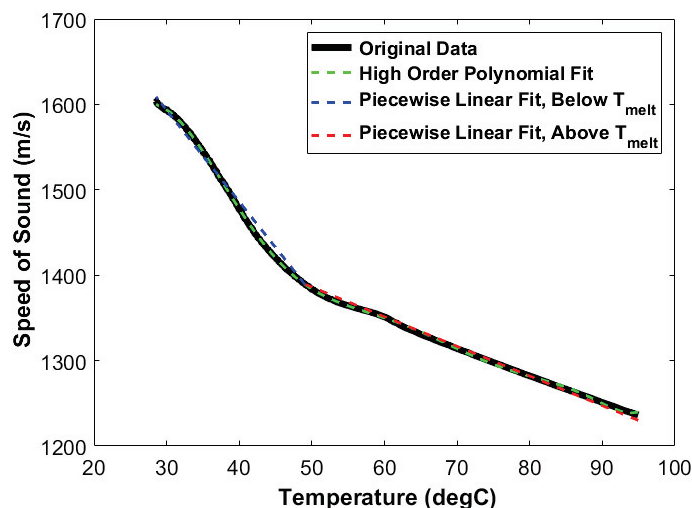

FIGURE 4. Speed of sound curve for CBL-125 from 30 to 95 degrees Celsius

There is a significant slope change between 40 and 50 degrees Celsius, the same range of temperatures that the melt was observed from the DSC results. The curve is well approximated by a single 8th order polynomial, but this is not used in the present study as it is susceptible to non-physical derivatives near the melt temperature that will cause issues in the inverse analysis discussed in the results section. In the present study the speed of sound as a function of temperature is approximated by piecewise, continuous function using two discrete linear lines that intersect at the melt temperature of 49°C, which is determined to be the melting temperature based on the optimization of the data and corresponds nicely to the DSC results. The linear piecewise function has an R-squared value of 0.9950, which is a very small deviation from the R-squared value of the high order polynomial fit (R-squared = 0.9999). In order to reduce the number of parameters necessary to use the speed of sound curve in later calculations, the piecewise linear fit is used to approximate the speed of sound curve.

With the material characterized for its acoustic behavior as a function of temperature, an experimental setup using a cylindrical geometry is constructed. A 16.5-centimeter diameter steel container is surrounded by eight 1" diameter Olympus 0.5 MHz transducers, which are held in place with a canvas belt, insulated from the container with a thin layer of Ultem, and coupled using an acoustic gel couplant. The eight transducers create four ultrasonic paths, at 45 degree intervals, with half the transducers acting as transmitters and half as receivers. An aluminum heating block, containing two 80 watt Watlow FIREROD Cartridge Heaters, is located centrally in the container, and a single line of thermocouples is used to gather internal temperature data directly, to be used to verify the ultrasonic results. The transducers are shown from a side view in Figure 5b along with the heater placed on the bottom of the container, but it is noted that the thermocouples are placed such that they are not all impeding the acoustic signals of any pulsar-receiver path, with the exception that one thermocouple is placed in the center of the container and any interference would equally effect all captured signals (Figure 5a).
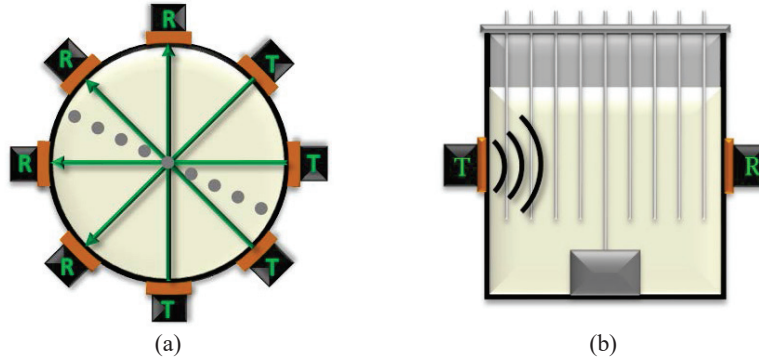

(a)   (b)

FIGURE 5. Cylindrical test set-up (a) top view and (b) side view

Experimental Procedure

The CBL-125 wax begins at ambient temperature, which is approximately 22°C. The heater is set to 81.6°C and turned on immediately after the data collection begins. The data from the thermocouples within the container is recorded throughout the test and is analyzed independently of the ultrasonic data. The heater is left on for 252 minutes before being turned off, and the CBL-125 is left to cool by convection with the surrounding air. No other external heating or cooling is applied during any part of the experimental process. After 300 minutes the experiment is terminated.

Data Collection

To collect the ultrasonic data, the authors created a custom LabVIEW virtual instrument. Data collection, once begun, is fully automated, including the adjustment of the electrical gain amplification to insure a clear signal throughout. This time varying gain is necessary as the ultrasonic signals attenuate differently throughout the test depending upon the current temperature of the material.

The operator of the LabVIEW virtual instrument sets the desired gain percent saturation, in this test that is chosen to be 80% of saturation, and the electrical gain is automatically adjusted so that the signal reaches that threshold each time data is collected. The custom LabVIEW virtual instrument offers full control of many different test parameters which can be set prior to collecting data. Users can define the number of active channels, the number of signals averaged for a single data set, the length of time to collect data for, the interval between data collection. Ultrasonic parameters, such as pulse width, sampling rate, low and high pass filters, and the DC offset are also controllable through the custom LabVIEW interface.

During data collection, the operator may inspect the current a-scan of any channel, but in the present study no changes were made to the setup once the test begun. Only the gain changes, and this automatically, to account for the attenuation within the wax. The raw data is collected as the experiment progresses, including the test parameters and a file which tracks the level of electrical gain for each channel. These files are analyzed in MATLAB, as is the data from the internal thermocouples recorded using the Graphtec GL820 Data Logger.

RESULTS AND DISCUSSION

Data Processing

The data collected through the LabVIEW virtual instrument is processed using custom MATLAB scripts. Each individual a-scans from each channel is placed through a custom filter tuned to the transducer to remove high and low frequency noise and a typical result is shown in Figure 6a. The signal onset is used to determine time of flight for the signal and is shown in Figure 6b. The material system begins at a room temperature of 22°C and is internally heated until 252 minutes into the test. The heater is then turned off and the wax is left to cool until the test ended at 300 minutes. The heater shut-off is clearly visible in the time of flight as indicated in Figure 6b. The effective speed of sound is calculated from the raw time of flight information using equation 1, and the results are shown in Figure 6c. The gain required to maintain an 80% signal threshold is also plotted as a function of time and is shown in Figure 6d. Notice from the gain that the required signal amplification decreases as the wax transitions to a liquid.
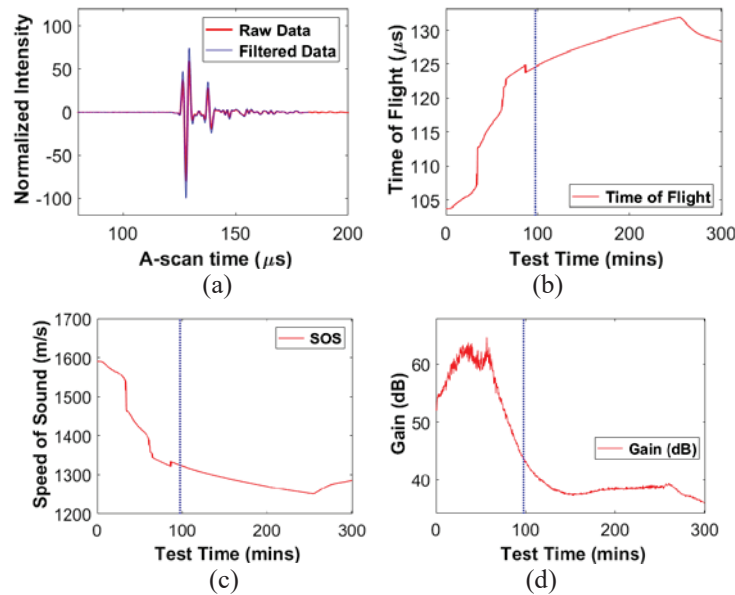

FIGURE 6. Data analysis and processing for a single channel (a) A-scan and filtered a-scan (b) Time of flight (c) Speed of sound (d) Gain

The normalized a-scan intensity can be formatted into a "b-scan" as a way of viewing a channel's a-scan signal over the entire test in a single image. Unlike a classical b-scan which plots a signal as a function of position, in the present context the b-scan is of the a-scan taken at various moments in time. This is shown in Figure 7 for the first channel. The signal at every moment in time is normalized to +/- 1 so as to view the waveform regardless of the material state of the wax. At the beginning of the text, the onset of the signal is viewed around 100 μs and this signal onset drifts to later moments in time. Notice the clear shift in the slope of the signal onset at 50 minutes, which corresponds to the time when the melt front starts to pass along the channel 1 acoustic front. At 250 minutes, there is a clear change in slope as the peak intensity begins to shift due to the absence of internal heating.
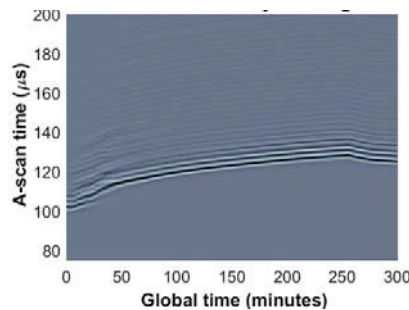

FIGURE 7. A-scan signal intensity over the experimental time for channel 1.

Thermocouple Temperatures

A line of thermocouples was used internally within in the CBL-125 as a method of verification as shown in Figure 5b. The temperature data recorded by the Graphtec GL820 Data Logger is shown in Figure 8 for each thermocouple as a function of time, with TC-1 and TC-5 being closest to the center of the bucket and TC-4 and TC-8 being furthest from the centerline.
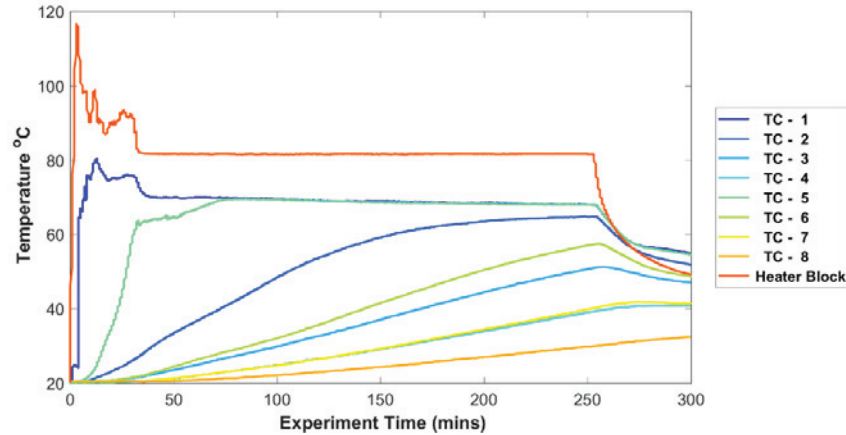

FIGURE 8. Thermocouple temperatures vs time.

From this information, as well as knowing the location of each thermocouple, an axisymmetric two-dimensional representation of the temperature across a plane of the container is created and shown in Figure 12a. The planar representation uses the average of a pair of thermocouples (e.g. TC-1 and TC-5) which are equidistant from the center of the container. That average temperature is then applied to all points at the radius corresponding to the thermocouple location, resulting in a circular temperature profile.

Ultrasonic Phase Change and Temperature Identification

Within the bucket along a single acoustic path the wave can pass through liquid, semi-liquid, semi-solid, and solid zones This is depicted in Figure 9 showing a radial projection from the bucket center where the wax is partially melted. We begin by assuming that the system is radially symmetric. This is not the same as axial symmetry, but it is assumed that for a given rotation angle about the center axis the wax phase state is periodic every 180º along a radial projection. When the entire bucket is fully solid or liquid, the temperature quantification is much simpler, the challenge is when multiple phase states exist within the same acoustic path. In the present model there are three states that the system is limited to, a temperature when the wax is either all solid or all liquid (Figure 10a), a center region of soft wax with an outer core of a solid wax (Figure 10b), and a center region of liquid wax with a soft zone and then a solid outer core. The temperature state of the wax on the surface of the bucket is assumed to be equal to that of the bucket outer surface as the conductivity of the metal bucket is much higher than that of the wax. In the presented set of results the temperature state of the bucket surface was not recorded, but a temperature profile of A boundary condition on the temperature of the wax is made on the outer bucket of the wax, and regardless of the state the wax is in within the bucket, it is assumed that the outer edge of the wax has the same temperature as the wall of the bucket.

In the scenario when the effective time of flight can be described, each can be related to the bulk speed of sound. In the first scenario, determined when the effective speed of sound is below a certain threshold, the wax is assumed to be completely solid and temperature state is assumed by the state shown in Figure 10a. Beyond this threshold, a profile is assumed where the wax is softening during the heating process, transitioning from solid to liquid, but is not yet liquid in any region across the ultrasonic path. Due to the amorphous nature of the wax, there is no single melt temperature, so the softening effect accounts for the range of temperatures over which the wax melts. The temperature profile can be depicted by the state shown in Figure 10b. The third state is when the wax is assumed to have some internal radius of melt and has a softening zone as shown in Figure 10c.
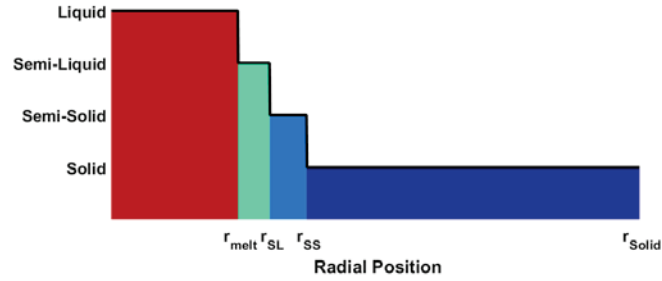
FIGURE 9. The three-step function approximation for phase of CBL-125

Using threshold limits that correlate the temperature and phase to speed of sound, an approximation for the phase of the CBL-125 over time can be created. Using the four ultrasonic paths, this approximation takes the form of a two-dimensional plane (Figure 12c).

In a similar method to the phase approximation, the temperature of the CBL-125 can also be approximated. First, multiple internal temperature profiles are assumed and approximated as piecewise functions based on the behavior of CBL-125 during heating and melting (Figure 11). For this experiment, the wax begins at a uniform temperature and fully solid (a). Knowing the speed of sound vs temperature master curve for CBL-125, softening is defined as occurring at the junction between the two linear functions from Figure 4. As the bulk speed of sound of the wax decreases, corresponding to an increasing temperature, there is a threshold at which the speed of sound cannot be obtained if the wax is fully solid, therefore it must have an internal soft zone of some radius. An optimization scheme is used to determine the radius of that soft zone based on the speed of sound master curve. The soft and solid regions are assumed to have a uniform temperature all the way through (b). As the wax continues to heat, the bulk speed of sound decreases further until it reaches a threshold where some portion of the wax must be liquid. The temperature of the liquid is approximated as 20 degrees Celsius above the melt temperature, for internal convection, and is assumed to be a uniform temperature. Outside of the melt region, the temperature is assumed to decrease linearly until it reaches the wall temperature (c). Then a two-dimensional plane is used to portray the temperature field across the wax (Figure 12b). During this experiment, the surface temperature at the boundary conditions must be assumed, however future experiments can capture the exact temperature profile of the surface using thermocouples or infrared technology.
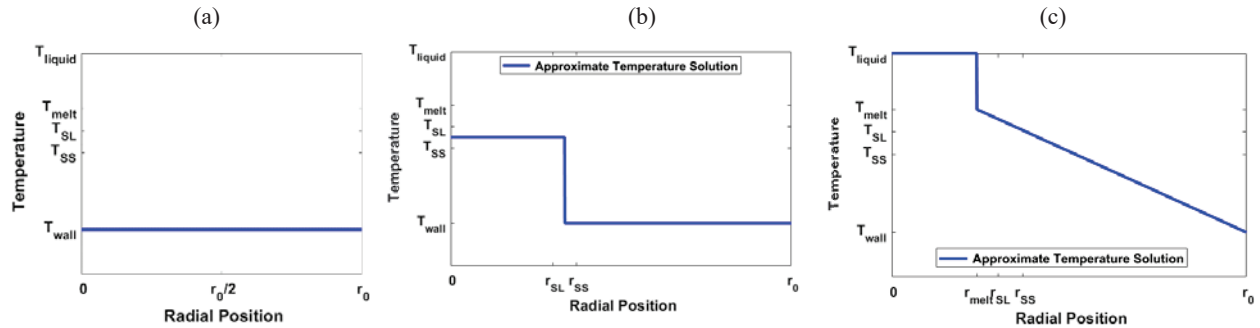

FIGURE 10. Three internal radial temperature profiles as approximated by piecewise functions (a) when fully solid (b) when heating and softening and (c) when partially melted

The assumed temperature and phase profiles are functional over all time and phases of the amorphous wax, and are applied to each channel separately. To achieve the 2D planar approximations shown in Figure 11b and 11c, the values between each channel location are approximated by interpolation.
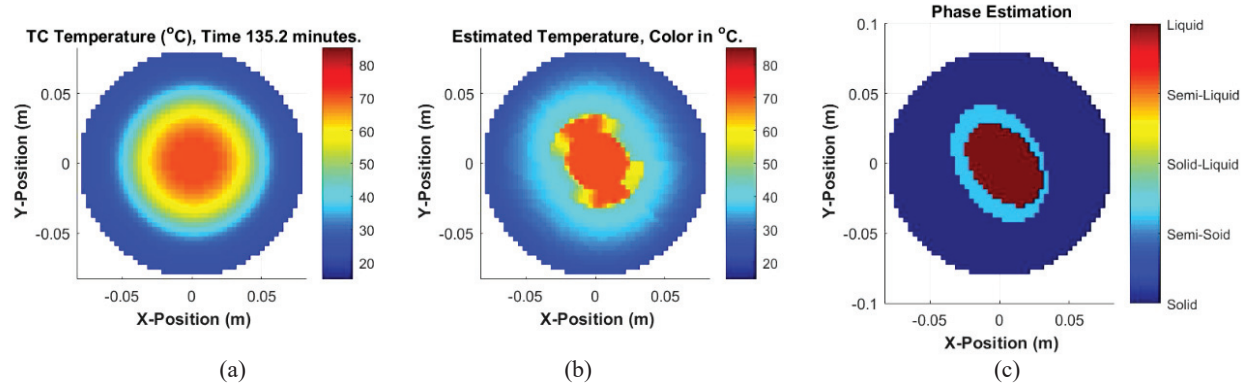
FIGURE 11. At 135 minutes (a) 2D temperature approximation using thermocouples (b) 2D temperature approximation using ultrasound (c) 2D phase approximation using ultrasound

At 135 minutes into the experiment, Figure 11b and 11c show the temperature and phase approximation based on the ultrasonic data. Figure 11a is the temperature profile from the thermocouples. Recall that the 2D temperature plane from thermocouple data is axisymmetric, resulting in a circular temperature profile. This differs from the ultrasonic 2D approximations, which interpolate between the channels (located every 45 degrees), permitting the non-circular geometry shown.

CONCLUSIONS & FUTURE WORK

The phase and temperature approximations across the container of CBL-125 can be created for the entirety of the experiment. Figure 12 shows three two-dimensional plots and the experimental setup, all at 252 minutes into the experiment.
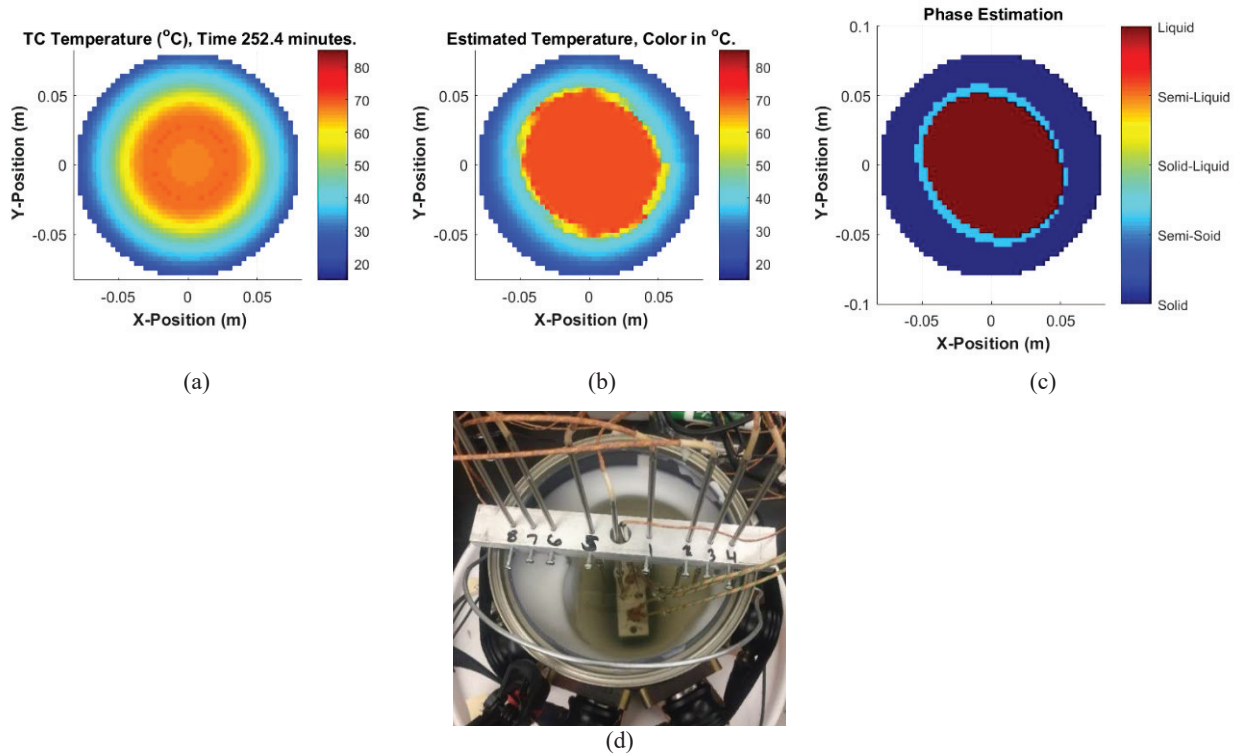

FIGURE 12. At 252 minutes (a) 2D temperature approximation using thermocouples (b) 2D temperature approximation using ultrasound (c) 2D phase approximation using ultrasound (d) Experimental setup

The agreement between the thermocouple approximation, the ultrasonic temperature approximation, the ultrasonic phase approximation, and a photo taken of the experimental setup at the same moment in time is quite good.

These results show that ultrasonics is a viable method for noninvasive phase and temperature identification. Additionally, the ultrasonic signals and subsequent analysis are not dependent on any prior ultrasonic data. Although this is a transient experiment, the results at a single moment in time are independent of the moments before and after. Sections of data can be analyzed independently of each other, without the need for any knowledge of the thermal history of the wax.

Discrepancies between the 2D temperature field from thermocouple data and ultrasonic data can be attributed to several factors: the thermocouples and the transducers are not on exactly the same plane; the thermocouple field is assumed to be axisymmetric and circular, which does not reflect the test setup exactly; the boundary conditions used for the ultrasonic analysis are approximated. These are all factors and issues which can be refined and addressed through further experimentation and analysis. The methods used here have applications in the food and beverage industry, petrochemical industry, and polymer composites industry. Internal material temperature and phase can be measured noninvasively for quality and system control.

Future work is focused on refining this method using measured boundary temperatures, implementation of these techniques to achieve a three-dimensional temperature reconstruction, and pursuing the scalability of these methods.

ACKNOWLEDGMENTS

REFERENCES

[1] R. Jia, Q. Xiong, G. Xu, K. Wang, and S. Liang, "A method for two-dimensional temperature field distribution reconstruction", *Appl. Therm. Eng.* **111**, 961 (2017).

[2] X Shen, Q Xiong, X Shi, K Wang, Sn Liang and M Gao, "Ultrasonic temperature distribution reconstruction for circukar area based on Markov radial basis approximation and singular value decomposition", *Ultrasonics* **62**, 174 (2015).

[3] M. Fujii and X. Zhang, "Noncontact measurement of internal temperature distribution in a solid material using ultrasonic computed tomography", *Exp. Therm. Fluid Sci.* **24**, 107 (2001).

[4] P.L. Schmidt, D. Greg Walker, D.J. Yuhas, and M.M. Mutton, "Thermal measurements using ultrasonic acoustical pyrometry", *Ultrasonics* **54**, 1029 (2014).

[5] N. Zhu, Y. Jiang, and S. Kato, "Ultrasonic computerized tomography (CT) for temperature measurements with limited projection data based on extrapolated filtered back projection (FBP) method", *Energy* **30**, 509 (2005).

[6] M. Takahashi and I. Ihara, "Ultrasonic monitoring of internal temperature distribution in a heated material", *Jpn. J. Appl. Phys.* **47**, 3894 (2008).

[7] M. Bramanti, E.A. Salerno, A. Tonazzini, S. Pasini, and A. Gray, "An acoustic pyrometer system for tomographic thermal imaging in power plant boilers", *IEEE Trans. Instrum. Meas.* **45**, 159 (1996).

[8] Y. Jia and M. Skliar, "Noninvasive ultrasound measurements of temperature distribution and heat fluxes in solids", *Energy Fuels* **30**, 4363 (2016).

[9] Y. Li, S. Liu and S.H. Inaki, "Dynamic reconstruction algorithm of three-dimensional temperature field measuremtn by acoustic tomography", *Sensors* **17**, 2084 (2017).

[10] C.B. Winkelmeyer, F. Peyronel, J. Weiss, and A.G. Marangoni, "Monitoring tempered dark chocolate using ultrasonic spectrometry", *Food Bioprocess Technol.* **9**, 1692 (2016).

[11] E. Hæggström and M. Luukkala, "Ultrasonic monitoring of beef temperature during roasting", *LWT - Food Sci. Technol.* **33**, 465 (2000).

[12] S.L. Stair, "Nondestructive Inspection and Characterization of Complex Engineering Materials via Ultrasound Techniques", Baylor University, 2017.

[13] C.M. Gregg, "The Observation of Phase State and Temperature Using Noninvasive Ultrasonic Waves", Baylor University, n.d.

[14] T. Russell, B.P. Heller., D.A. Jack, D.E. Smith, "Prediction of the fiber orientation state and the resulting structural and thermal properties of fiber reinforced additive manufactured composites fabricated using the big area additive manufacturing process", *Journal of Composites Science*, 2(2), **26**, (2018).

[15] B.P Heller, D.E. Smith, D.A. Jack, "Simulation of planar deposition polymer melt flow and fiber orientation in fused filament fabrication", *Journal of Additive Manufacturing*, **12**, Part B, 252-264, (2016)

[16] L.J. Love, V. Kunc, O. Rios, C.E. Duty, A.M. Elliot, Journal of Materials Research, suppl. Focus Issue: The Materials Science of Additive Manufacturing, **29**(17), 1893-1898, (2014).

[17] L.W. Schmerr, Fundamentals of Ultrasonic Nondestructive Evaluation: A Modeling Approach (Plenum Press, New York, 1998).

[18] C.D. Motchenbacher and J.A. Connelly, Low Noise Electronic System Design (J. Wiley & Sons, New York, 1993).